Few-Atom Silver Clusters as Fluorescent Reporters

Isabel Díez and Robin H.A. Ras

Abstract Silver clusters, composed of only a few silver atoms, have remarkable optical properties based on electronic transitions between quantized energy levels. They have large absorption coefficients and fluorescence quantum yields, in common with conventional fluorescent markers. But importantly, silver clusters have an attractive set of features, including subnanometer size, nontoxicity and photostability, which makes them competitive as fluorescent markers compared with organic dye molecules and semiconductor quantum dots. In this chapter, we review the synthesis and properties of fluorescent silver clusters, and their application as bio-labels and molecular sensors. Silver clusters may have a bright future as luminescent probes for labeling and sensing applications.

Keywords Fluorescent marker · Nanoclusters · Nanodots · Nanoscale metal · Quantum dots

Contents

I. Díez, and R.H.A. Ras (✉)
Department of Applied Physics, Aalto University (formerly Helsinki University of Technology), Puumiehenkuja 2, FI-02150 Espoo, Finland
e-mail: robin.ras@tkk.fi

A.P. Demchenko (ed.), *Advanced Fluorescence Reporters in Chemistry and Biology II: Molecular Constructions, Polymers and Nanoparticles,* Springer Ser Fluoresc (2010) 9: 307–332,
DOI 10.1007/978-3-642-04701-5_10,

1 Introduction

Luminescence of silver by quantum confinement has been known for several decades e.g., silver clusters in zeolites [1–3], in cryogenic noble gas matrices [4, 5], in inorganic glasses [6–8] and in silver oxide films [9–11]. In the 1980s and 1990s, silver clusters could be prepared in aqueous solution, often using radiolysis, however they were rather unstable and their luminescence was not reported [12–14]. For example, Henglein wrote about "long-lived" silver clusters that live "for many hours" [14, 15]. Obviously, for many practical applications a lifetime of hours is not sufficient. Stable aqueous solutions containing small silver clusters and their luminescence were reported in 2002 in the pioneering work by Zheng and Dickson [16]. Meanwhile, silver clusters have gained importance [17], and basically two kinds of applications have been explored: (1) their use as fluorescent labels for microscopic imaging, and (2) their use as fluorescent probes in molecular sensing.

In general, silver clusters in solution are prepared by reduction of silver ions. Proper scaffolds, e.g., DNA, proteins, dendrimers and polymers, are essential to prevent the aggregation of clusters to larger nanoparticles. Although it is clear that the emission originates from few-atom silver clusters, many aspects of this exciting class of nanoscopic metals are not yet fully understood.

Current fluorescence applications mostly involve organic fluorophores (e.g., rhodamine dyes) or semiconductor quantum dots (e.g., CdSe), both have their own weaknesses and strengths (see Table 1). For example organic fluorophores exist in a wide range of chemical structures and spectral properties; however, their main weakness is that they are prone to photobleaching. On the other hand, semiconductor quantum dots are photostable; however, their large physical size may hinder their use as fluorescent reporters of binding events and, in addition, they are toxic, which may compromise their use for in-vivo applications. Silver clusters combine their positive properties. They are extremely bright, photostable, and nontoxic, have a subnanometer size, and do not blink at time scales relevant for biological applications (0.1 ms–1 s) [18, 19]. These properties allow their use even in single-molecule studies [19]. Recently, Ras et al. demonstrated that silver

Table 1 Comparison of silver clusters with conventional fluorophores [18]

	Silver clusters	Organic dyes	Semiconductor quantum dots
Size	$<$1 nm	$\sim$1 nm	10–20 nm
Photostability	Stable	Bleaches	Stable
Toxicity	Nontoxic	Toxic/nontoxic	Toxic
Blinking	No	Yes	Yes

clusters exhibit electrogenerated chemiluminescence (also called electrochemiluminescence) [20]. In summary, silver clusters have an appealing set of features that complements the conventional fluorophores.

In this chapter, we discuss first how the silver clusters relate to silver atoms and silver nanoparticles. Then we overview the formation of fluorescent silver clusters in aqueous solution, using silver salts as precursors and various scaffolds as stabilizers. Finally we discuss applications of silver clusters in fluorescent labeling of biological tissues, and their use as fluorescent probes for sensing of molecules.

2 Metal Clusters: The Missing Link Between Single Atoms and Plasmonic Nanoparticles

The behavior of metals goes through several noticeable transitions when their size is varied (Fig. 1). Metals of macroscopic dimensions, such as silver jewelry and copper wires, have a mirror-like luster and are good electrical conductors. This

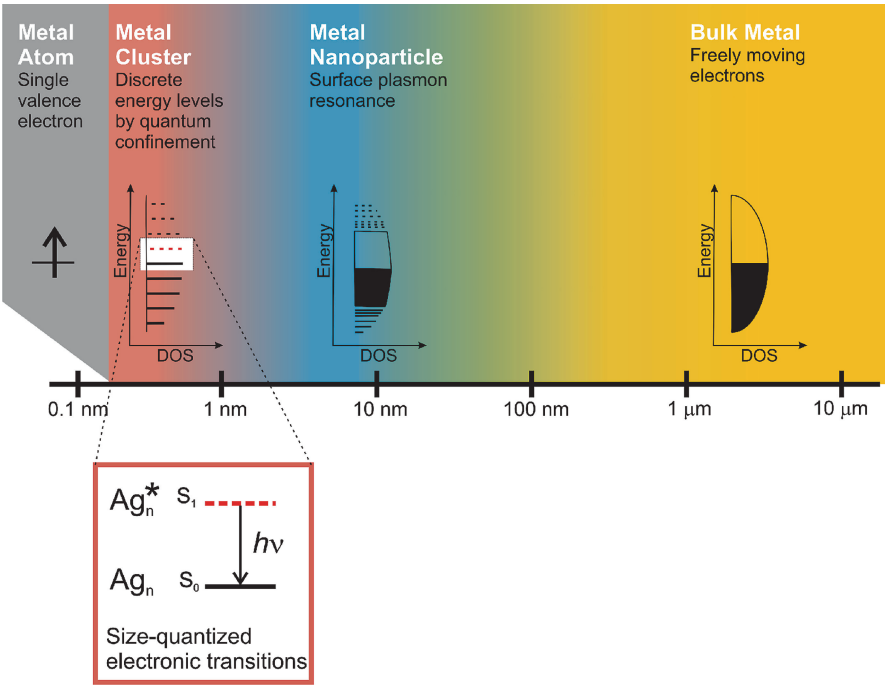

Fig. 1 The effect of size on metals. Whereas bulk metal and metal nanoparticles have a continuous band of energy levels, the limited number of atoms in metal clusters results in discrete energy levels, allowing interaction with light by electronic transitions between energy levels. Metal clusters bridge the gap between single atoms and nanoparticles. Even though in the figure the energy levels are denoted as singlets, we must remark that the spin state of the silver clusters is not yet firmly established

behavior finds its origin in that the atoms in bulk metal share their valence electrons into a homogeneously distributed sea of freely moving electrons. In bulk metal, the energy levels of the electrons are squeezed to such an extent that they appear as a continuum. As metals do not have a band gap between the valence band and the conduction band, electrons do not experience a barrier to populate the conduction band. In bulk, the scattering of the electrons is determined by the electron mean free path, which is 52 nm in the case of silver [21].

When the size of metals is comparable or smaller than the electron mean free path, for example in metal nanoparticles, then the motion of electrons becomes limited by the size of the nanoparticle and interactions are expected to be mostly with the surface. This gives rise to surface plasmon resonance effects, in which the optical properties are determined by the collective oscillation of conduction electrons resulting from the interaction with light. Plasmonic metal nanoparticles and nanostructures are known to absorb light strongly, but they typically are not or only weakly luminescent [22–24].

Further reduction of the particle size down to 1 nm or less leads to breaking up of the band structure into discrete energy levels because the number of atoms becomes limited. The metal at this small scale is called a metal cluster and is not a conductor any more, as the energy levels are too far separated. Therefore, the collective oscillation of electrons is also obstructed and the metal cluster is not plasmonic. Interaction with light is still possible though, via electronic transitions between the energy levels, similar as in organic dye molecules. The metal clusters have a molecule-like behavior. The physics behind few-atom metal clusters is well described in the review by Dickson and coworkers [25]. The nanoclusters of gold and their biolabeling applications are described in the chapter of Muhammed and Pradeep [78].

3 Terminology

The materials described in this chapter are denoted in the literature mostly as “metal clusters” or “metal nanoclusters”. However, the terminology “metal clusters” spans various scientific disciplines and has consequently multiple meanings, including plasmonic nanoparticles and various nanosized metallic structures. Therefore alternative names have been given, although they are at the moment supported only by a fraction of the scientific community: quantum clusters [26], nanodots [27], metal quantum dots [25] and superatoms [28].

A clear, commonly accepted terminology to describe few-atom subnanoscale metals exhibiting quantized energy levels is lacking. The lack of a coherent terminology leads to confusion and may hamper development. In this chapter, we restrict the term “*metal cluster*” to describe few-atom metals with discrete energy levels, and use “*metal nanoparticle*” for particles that have surface plasmon resonance effects (approximate size range between 1 and 100 nm).

The quantized silver clusters can be considered as “metal quantum dots”, because these are zero-dimensional materials where the band gap is formed by

quantum confinement. The silver clusters can also be considered as a "superatom", since they may have a clear valence electron shell structure, similar as the electrons in ordinary atoms.

4 Synthesis of Fluorescent Silver Clusters in Various Scaffolds and Their Application as Bio-Labels

Silver clusters in solution are prepared by reduction of silver ions in the presence of proper scaffolds, including DNA, proteins, dendrimers and polymers. The scaffolds typically have multiple groups that allow strong interaction with silver ions, such as complexation with DNA bases or ionic interactions with acrylate polymers. The formation of clusters requires suitable conditions to avoid aggregation of the clusters into larger nanoparticles, such as the initial ratio silver:scaffold, the overall concentration, or the type of reductant. Even though many recipes exist for silver clusters in solution, it is not yet understood why the accumulation of silver atoms stops at the size of few-atom clusters. The reduction of silver ions to silver clusters is carried out mainly by two methods, by using a chemical reductant, for instance sodium borohydride, or by photoactivation, i.e., reduction initiated by ultraviolet light [29, 30] or visible light [9, 31]. Furthermore, recent developments and potential applications of fluorescent silver clusters as fluorophores in the field of bio-imaging will be described.

4.1 DNA Oligonucleotides

The strong attraction of silver ions for DNA bases allows the use of these as templates for the formation of silver clusters (Fig. 2a), but special care is needed to avoid the formation of larger nanoparticles [33–39]. It is known that silver ions bind preferentially the heterocyclic bases and not the phosphates [40–42] and prefer the single-stranded DNA (ssDNA) over the double-stranded DNA [43–45].

In this section, the complexity encountered in the design of a proper oligonucleotide as template for the formation of highly luminescent and very stable silver clusters will be shown. Some of the templates discussed in literature are summarized in Table 2.

The first silver clusters made using DNA as template were reported by Dickson et al. in 2004 [32]. The paper describes the time-dependent formation of silver clusters in a 12-base (5′-AGGTCGCCGCCC-3′). The clusters have intense absorption in the region 400–550 nm (Fig. 2b) and emission at around 630 nm. The latter band could be decomposed as the emission bands of two distinct excitations at 540 and 580 nm, indicating the existence of two different emitters. As the clusters do not have inherent chirality, the induced circular dichroism associated with the silver cluster electronic transitions is evidence that the clusters are bound to DNA (Fig. 2c).

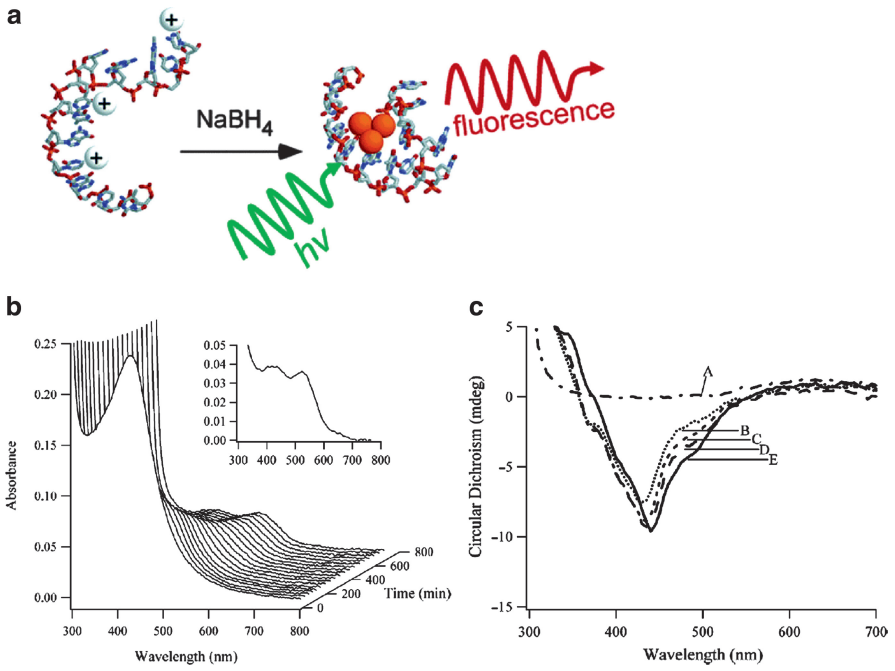

Fig. 2 (**a**) Schematic of the formation of silver clusters using DNA oligonucleotide as scaffold. After complexation of DNA with silver cations, the mixture is reduced with $NaBH_4$ and the fluorescent cluster is formed. (**b**) Absorption spectra of silver clusters acquired every 30 min using [5′-AGGTCGCCGCCC-3′] = 10 μM, $[Ag^+]$ = 60 μM, and $[BH_4^-]$ = 60 μM. The foremost spectrum was acquired 9 min after adding the BH_4^-, and it has λ_{max} at 426 nm. The *inset* spectrum shows the last spectrum in the series (692 min), with peaks at 424 and 520 nm. (**c**) Induced circular dichroism spectra. The cell path length was 5 cm. The spectra were collected 2 min (A, *dashed-dotted line*), 20 min (B, *dotted line*), 40 min (C, *fine dashed line*), 60 min (D, *coarse dotted line*), and 150 min (E, *solid line*) after adding the BH_4^- [32]

Although the final stoichiometry of the solution was 2:1:1 in bases:Ag^+:BH_4^-, the complexes formed have a maximum of 4 Ag^+ or 4 Ag atoms per DNA strand, as demonstrated by electrospray ionization mass spectrometry. This stoichiometry was explained as an end-effect of the short oligonucleotide. Moreover, ^{1}H NMR indicates that silver interaction with cytosine base is stronger than with other bases.

This was the starting point of further studies on the formation of silver clusters in oligonucleotides, for example in a 12-mer cytosine (5′-CCCCCCCCCCCC-3′; also denoted as dC_{12}). Using the same stoichiometry, 2:1:1 in bases:Ag^+:BH_4^-, emission spectra recorded at various excitation wavelengths reveal the presence of multiple electronic transitions with emissions centered at 485 nm, 525 nm and 665 nm, this last one, from two different excitations (Fig. 3a). The evolution in time after addition of the reductant shows an isosbestic point with a decrease in the emission band at 665 nm and an increase of the bands at ∼500 nm, suggesting a chemical transformation between the emitters, at least at pH lower than 10

Table 2 Oligonucleotide sequences used as templates for the formation of silver clusters

Template sequence	Emission max (nm)	Φ_F (%)	Ref.
5′-CCCTTTAACCCC-3′	485	–	[46]
5′-CCCTCTTAACCC-3′	520	16.3	[46]
5′-CCCTTAATCCCC-3′	572	28.2	[46]
5′-CCTCCTTCCTCC-3′	620	32.4	[46]
5′-AGGTCGCCGCCC-3′	630	–	[32]
5′-CCCATATTCCCC-3′	660	18	[47]
5′-CCCTATAACCCC-3′	680	37	[47]
5′-CCCTAACTCCCC-3′	710	31	[47]
dC_{12}	700, 665, 485, 525	17	[19, 48]
$dC_4T_4C_4$	495	–	[49]
$dT_4C_4T_4$	475	–	[49]
dT_{12}	540	–	[49]
dC_{24}	634	–	[50]
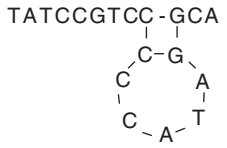	648	–	[45]
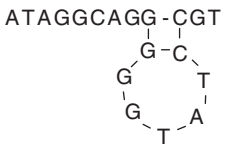	574	–	[45]

Φ_F Fluorescence quantum yield, C cytosine, G guanine, A adenine, T thymine

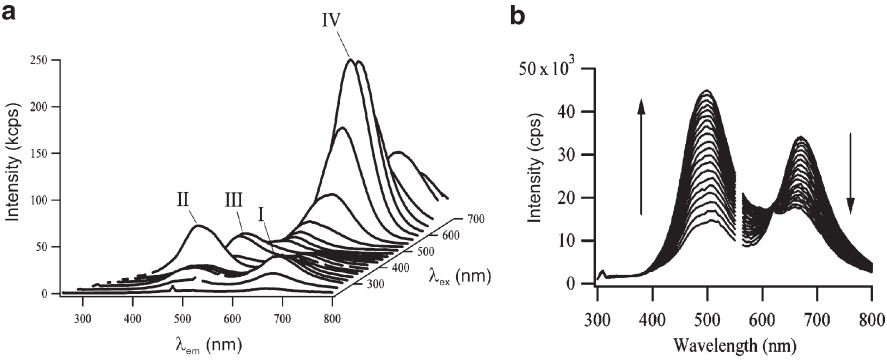

Fig. 3 (**a**) Fluorescence emission spectra (*bottom axis*) as a function of the excitation wavelengths (*right axis*), for silver clusters prepared with the molar ratio dC_{12}:Ag^+:BH_4^- of 1:6:6. The spectra were acquired 4.5 h after adding the BH_4^-. The dominant emission band occurs at (IV) $\lambda_{ex} = 580$ nm/$\lambda_{em} = 665$ nm. Three other bands occur at (I) $\lambda_{ex} = 280$ nm/$\lambda_{em} = 665$ nm, (II) $\lambda_{ex} = 340$ nm/$\lambda_{em} = 485$ nm and (III) $\lambda_{ex} = 440$ nm/$\lambda_{em} = 525$ nm. (**b**) Time evolution of the fluorescence emission spectrum using $\lambda_{ex} = 280$ nm, which excites both the red- and green-emitting species. The isosbestic point at 615 nm, results as the intensity at 495 nm increases, while the intensity at 670 nm decreases. Spectra collected every 30 min starting 3 h after adding the BH_4^- [48]

(Fig. 3b). The conversion of red emitters into green emitters with time was explained as an oxidation reaction confirmed by the addition of extra reductant, which leads to the transformation of green emitters into red ones [48].

There are several publications describing the role of DNA bases and base sequence on the formation of fluorescent silver clusters. The different bases have different affinity for silver and the different base-silver cluster interaction produces different emissions. For a given DNA strand, every particular base sequence creates a different environment for the clusters and consequently a different emission. For instance, Petty et al. have studied the influence of thymine (T) and cytosine (C) bases by playing with their combinations in oligonucleotides [49]. Fluorescent silver clusters formed in dT_{12} and $dT_4C_4T_4$ have similar properties. The emission intensity increases with pH having a midpoint at pH 9.5, which is close to the pK_a of the N3 of thymine indicating that the deprotonated thymine forms a complex with the fluorescent silver clusters. In nitrogen atmosphere, nonfluorescent clusters are formed, whereas the presence of oxygen allows the formation of fluorescent species, which suggests in this case that nonfluorescent species are reduced while fluorescent ones are oxidized. A ratio bases:Ag^+ of 2:1 leads to a maximum in the emission intensity when using both templates, dT_{12} and $dT_4C_4T_4$, interpreted by the authors as the same cluster size is stabilized by both oligonucleotides. Silver clusters show similar excitation maxima, but different Stokes shifts, pointing out the role of the bases and their influence on the environment of the clusters and therefore on the optical properties of the clusters. In the case of more cytosine-rich oligonucleotides such as $dC_4T_4C_4$ similar properties were found but an additional emitter was formed here, a red emitter.

Dickson et al. carried out a high-throughput analysis of 12-mer DNA strands and found that the cluster properties are highly sequence-dependent, claiming that discrete sequences lead to well defined silver clusters sizes and hence to distinct emission properties ranging from visible to near-IR [46]. Three long-wavelength emitters, yellow, red and near-IR, were prepared in oligonucleotides and presented as good candidates for their use as single molecule biolabels (Fig. 4). The synthesis of each of the emitters in oligonucleotides does not follow a general procedure, since the optimal synthetic conditions differ for every case, for instance regarding the use of buffered or unbuffered solutions and pH closer to 5 or to 8. However, the efforts are rewarded since silver clusters protected by oligonucleotides present many advantages, especially those emitting in the near-IR. For instance, these clusters can be excited with low energy, which is beneficial for the photostability of the clusters and preserves the chemical stability of the scaffold. Moreover, biological samples have low background fluorescence signals in the near-IR, providing high signal-to-noise ratio. These silver clusters present large absorption coefficients and quantum yields exceeding 30% (Table 2). Compared to cyanine dyes, these emitters have higher emission intensities (1,500 and 2,500 counts/s for cyanine dyes and clusters respectively, Fig. 5) and longer lifetimes (decay to $1/e$ emitters in 9 and 580 s respectively) [46]. They do not blink in relevant timescales (0.1–1,000 ms) and the dark-state lifetime of 30 μs can be reduced to less than 10 μs by increasing the intensity of the excitation [19].

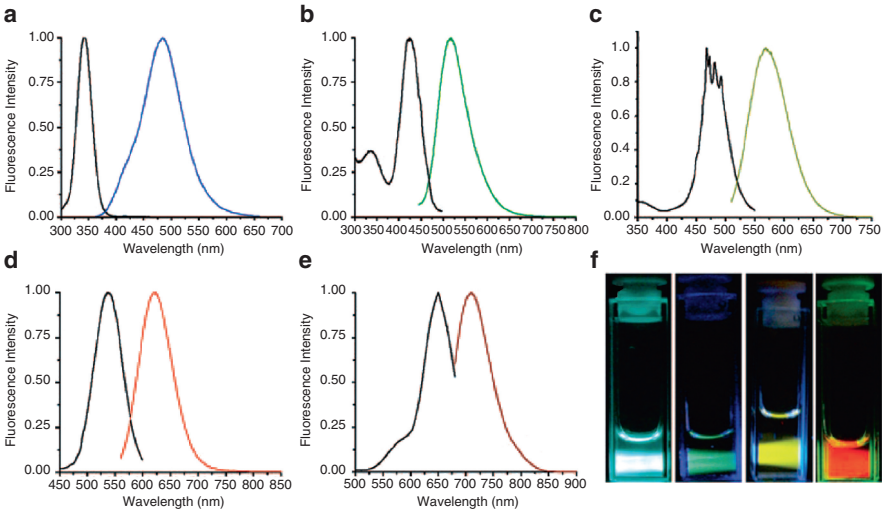

Fig. 4 Steady-state excitation and emission spectra for five distinct ssDNA encapsulated Ag clusters. (**a**) Blue emitters created in 5′-CCCTTTAACCCC-3′, (**b**) green emitters created in 5′-CCCTCTTAACCC-3′, (**c**) yellow emitters created in 5′-CCCTTAATCCCC-3′, (**d**) red emitters created in 5′-CCTCCTTCCTCC-3′, and (**e**) near-IR emitters created in 5′-CCCTAACTCCCC-3′. (**f**) Pictures of emissive solutions in (**a**)–(**d**) [46]

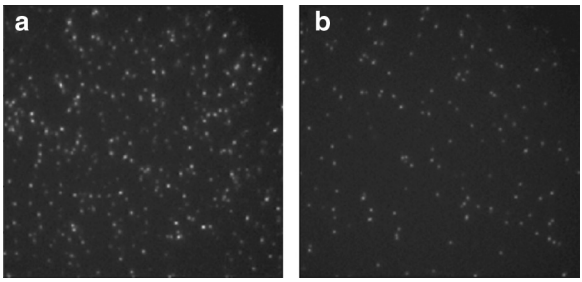

Fig. 5 (**a**) Image of single IR-emitting dC_{12}–Ag_n molecules in a poly(vinyl alcohol) (PVA) film. (**b**) Image of single Cy5.29 molecules in a PVA film. The image dimensions are 40 × 40 μm, and imaging conditions of (**a**) and (**b**) are identical [19]

Recently it was shown that optical modulation of the silver cluster fluorescence could allow extracting weak signals from extremely fluorescing backgrounds. The method consists in coillumination with an intensity-modulated secondary laser (excitation ~800 nm) and produces a photobrightening of higher energy cluster emissions by depopulation of the dark state without increasing the background (Fig. 6a, b) [27]. In this way, silver clusters with emission at ~710 nm (upon excitation at 633 nm) can be distinguished from background signals created by autofluorescence (Fig. 6c, d) or dyes (Cy5) (Fig. 6e, f) [27].

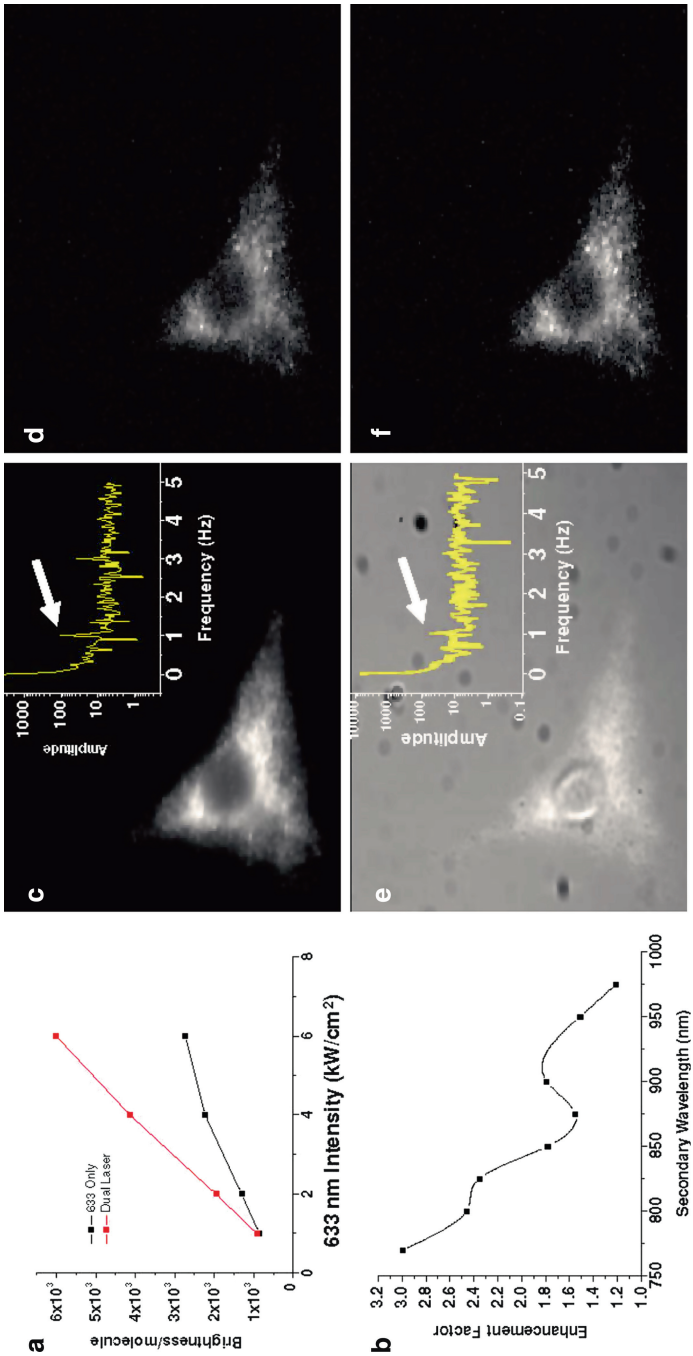

Fig. 6 (**a**) Brightness per Ag cluster under single-laser (633 nm, *black*) and dual-laser (633 nm + 805 nm, *red*) excitation, as determined by fluorescence correlation spectroscopy. Simultaneous 805 nm excitation (8 kW/cm^2) recovers the linearity between excitation and 710 nm emission. (**b**) Excitation scan of the secondary laser-based enhancement (4 kW/cm^2) relative to single laser excitation (633 nm, 1.2 kW/cm^2). (**c**) Typical dual-laser ccd image of biotinylated NIH 3T3 cells surface-labeled with avidin and biotinylated Ag cluster. The secondary laser modulates the fluorescence at every pixel simultaneously. *Inset*: Fourier transform of a typical pixel intensity as a function of time. (**d**) Autofluorescence is removed from the recovered cell image after demodulation at the modulation frequency [indicated by the *arrow* in the *inset* of (**c**)]. (**e**) Image of the same cell with highly concentrated Cy5 solution added to simulate a very high autofluorescent background. *Inset*: the modulation frequency remains readily apparent in the Fourier transform of a typical pixel intensity vs. time. (**f**) Demodulated image showing the nearly complete elimination of the Cy5 and autofluorescent background signals, leaving only the distinct signal of Ag clusters [27]

Additional studies confirmed the sequence dependency on the generation of fluorescent silver clusters when using scaffolds of 19 bases, with a shape of a hairpin or containing two single-stranded (C or G rich) sequences bound by two base pairs (Table 2). In this case, the authors claim that based on mass spectra, silver binds with comparable affinities to chemically similar sites on C and G bases. The reason for the differences in the emission peaks might be the unique local environment offered by different base stacking between the two strands or by distinct of the strand, since the incorporation of silver in the loop of the hairpin is more difficult than in the open geometry. The discrepancy regarding the silver-oligonucleotide affinity described by various groups could be also explained considering the different relative concentrations used in the experiments. Authors claiming higher affinity of silver for cytosine have used 0.5 silver per nucleotide, whereas authors claiming similar affinities for cytosine and guanine have used 0.29 silver per nucleotide and the preferences of silver might be different at different ratios [43, 44, 51, 52].

The fluorescence properties and stability of silver cluster in hairpins were reported to be related to the number of cytosines in the loop (varying from 3 to 12 cytosines) [53]. However, as a general rule, red emitters were brighter than green emitters. Further specific studies on the 9C loop show that the red emitter corresponds to Ag_{13}:DNA and the green emitter correlates with Ag_{11}:DNA. A great advantage of silver clusters encapsulated in hairpins is that they are bright enough to be imaged by using an epifluorescence microscope.

The high fluorescence quantum yield of DNA-encapsulated silver clusters ($\Phi_F > 30\%$) [46, 50] makes them good candidates as fluorophores in cell imaging. Aiming the application for cell imaging, the DNA-encapsulated silver clusters were prepared as described before but using a longer strand, a 24-mer oligocytosine (dC_{24}), linked to a protein, avidin. The presence of avidin does not affect the chemical or photophysical stability of the clusters (emission maximum at 634 nm, excitation at 580 nm, fluorescence lifetime of about 2.86 ns and remarkable brightness).

First results in this research showed that biotinylated fixed cells became fluorescent upon staining with avidin-dC_{24}-Ag clusters (Fig. 7a, b). However, in the case of living cells, loading with avidin-dC_{24}-Ag clusters produces bright spots, indicating endocytosis (Fig. 7c). The results were quite different when using an antibody, heparin sulfate (HS) instead of avidin. HS-dC_{24}-Ag clusters can penetrate the cells when incubated at 37°C showing fluorescent nuclei (Fig. 7d–f) [50].

4.2 Proteins and Peptides

A commonly used staining method for the cell nucleolus is based on silver nanoparticles [54]. The proteins of the nucleolus, such as nucleolin, are known to have high affinity to silver ions due to their amino-terminal domain. Subsequent reduction leads to the formation of the silver nanoparticles stain. In spite of all the efforts, a general and definitive conclusion regarding the attraction between silver

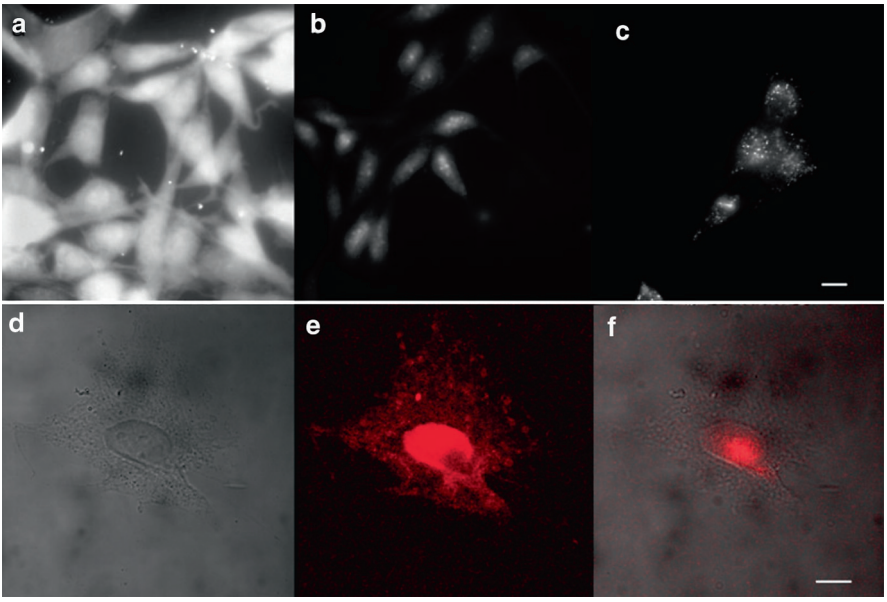

Fig. 7 (**a**)–(**c**) Fluorescence images of NIH 3T3 cells stained with Avidin-dC_{24}-Ag. (**a**) Fixed cells, biotinylated. (**b**) Fixed cells, nonbiotinylated. (**c**) Live cells, biotinylated. Images were recorded on a Zeiss Axiovert 200 microscope with a CoolSNAP CCD camera (Roper Scientific). Scale bar 30 μm. (**d**)–(**f**) Fluorescence images of live NIH 3T3 cells stained with anti-HS-dC_{24}-Ag. Live cells incubated with anti-HS-dC_{24}-Ag at 37°C for 6 min (**d**, bright field; **e**, silver clusters; **f**, merge). Images were recorded on Zeiss LSM 10 confocal microscope. The fluorescence images were taken at 543 nm excitation. Scale bar 25 μm [50]

ions and peptides cannot be easily extracted. In addition to the silver binding amino groups, some authors have demonstrated higher degree of silver binding in peptides rich in proline and hydroxyl residues [55], whereas others showed a preferential affinity of silver for methionine-containing peptides compared to their nonmethionine containing counterparts [56].

In 2007, Dickson et al. found that it is possible to stain fixed cells with fluorescent silver clusters instead of silver nanoparticles by tuning the staining conditions [57]. The new approach consists of staining fixed cells with a low concentrated silver nitrate solution 20–100 mM, within 20 h at ambient conditions, and reducing the silver by photoactivation, with the result of small silver clusters that present a broad emission band between 500 and 700 nm (Fig. 8a–d). The discovery that fluorescent silver clusters can be generated by photoactivation of cells fed with silver salt, opens up new paths for the application of silver clusters in biological systems.

Besides the formation of luminescent silver clusters in fixed cells, likely due to the presence of proteins, fluorescent silver clusters have been synthesized using proteins as templates. In 2008, Pal et al. reported on the use of an enzyme, bovine pancreatic α-chymotrypsin (CHT) as biotemplate during the chemical reduction of

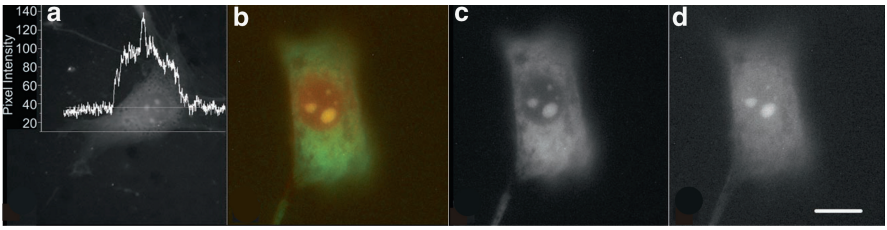

Fig. 8 Emission from formaldehyde-fixed NIH3T3 cells loaded with 100 mM silver nitrate for 20 h. (**a**) Fluorescence image; the *inset* is the intensity profile along the line drawn across the cell. (**b**) Merge of (**c**) and (**d**). (**c**) Emission from RNASelect fluorescence (*green channel*); (**d**) Emission from silver clusters (*red channel*); Scale bar 30 μm [57]

silver ions to produce well dispersed and stable solutions of protein-conjugated fluorescent silver clusters [58]. The protein-protected silver clusters show emission at 680 nm when excited at 500 nm. The molar ratio of CHT:Ag^+:BH_4^- was 1:10:100, where the large excess of $NaBH_4$ provokes two adverse effects in the system. A first consequence of the excess of $NaBH_4$, is that the reductant cleaves disulfide bonds inducing denaturation of the protein. Partial reconstitution of the protein was achieved with efficient oxidation, by dialyzing the sample against water of pH 8.0–8.5 for 24 h in aerated conditions. The functional integrity of the protein was confirmed by studying the enzymatic activity on a substrate Ala-Ala-Phe 7-amido-4-methyl coumarin. The enzymatic activity of CHT–Ag was retarded by 2.8 times compared to the activity of native CHT. The origin of the retard might be the reduction and oxidation processes since reconstituted CHT presents similar delays. This indicates that silver clusters are not located in the enzymatic active site of CHT. A second event caused by the excess of sodium borohydride is the increase in the pH and a subsequent aggregation of the protein. However, the aggregation might be reversible by lowering the pH with an exhaustive dialysis against pure water.

Prior to these findings, in 2005, fluorescent silver clusters in combination with a fluorophore, thioflavin T (ThT), were already used to image proteins [31]. Silver clusters were prepared by photoreduction at ~330 nm of solutions containing ThT and Ag^+. The emission band centered at ~450 nm grew by fivefold when ThT:Ag^+ was 100:1 and by 50-fold when the ratio was 1:1 (Fig. 9a, b), suggesting the enormous effect of silver. The authors proposed that the emission observed is originated by both, intrinsic formation of fluorescent silver clusters (when the samples were irradiated at 500 W/cm^2) and by metal-enhanced fluorescence of ThT (with irradiation at 1 W/cm^2). Amyloid fibrils stained with ThT-Ag clusters present a time-dependent increase of fluorescence with no photobleaching after 24 h of illumination at 475 nm (500 W/cm^2) in contrast to ThT-stained fibrils, which have a rapid decay of fluorescence (Fig. 9c). With this method, the authors managed also to image a single fibril and claim that the luminescence produced by ThT-Ag clusters is at least 100-fold higher than the luminescence reported in photoreduced silver clusters formed in water solution with dendrimers [16] or in Ag_2O films [9].

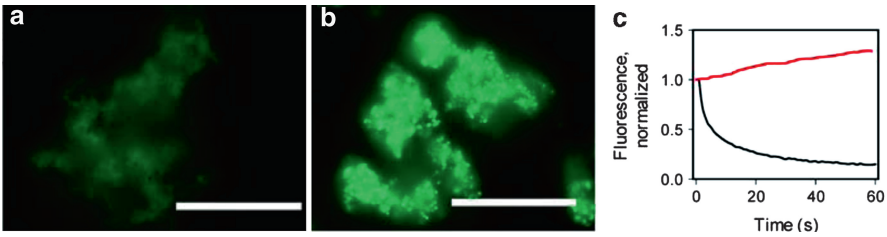

Fig. 9 Epifluorescence microscopy images of the amyloid fibrils of PrP 90–231 (1 μM), stained at room temperature with (**a**) ThT alone (10 μM) (exposure time 1.6 s), and (**b**) with preformed ThT-Ag clusters (exposure time 0.02 s). ThT-Ag clusters were preformed by irradiation of aqueous solutions of ThT (10 μM)/$AgNO_3$ (1 μM) at 312 nm for 3 min. Scale bars = 10 μm. (**c**) Photobleaching kinetics of the fibrils stained with ThT (*black line*) vs. photoactivation kinetics of the fibrils stained with ThT-Ag clusters (*red line*). Data collected from a 5 μm × 5 μm area and normalized to the intensity measured at zero time [31]

Taking advantage of the well-established affinity of silver cations for proteins as shown before in the case of nucleolin and due to the importance of nucleolin in actual investigations [59, 60], synthetic peptides derived from nucleolin were used as scaffolds for the formation and protection of fluorescent silver clusters [57]. The earliest peptide mentioned in literature as template for the formation of fluorescent silver clusters was the histidine-rich AHHAHHAAD, but synthesis and optical properties were only briefly described since that was not the main topic of the publication [61]. The first detailed study of peptides as scaffold [57] describes oligopeptides that contains 15–18 amino acids, including the most abundant amino acids in nucleolin, like glutamic acid (E), lysine (K), and aspartic acid (D) as well as cysteine (C), which is minor in nucleolin but it is known to bind silver [62]. The resulting peptide allows formation of silver clusters by reducing a silver solution (0.22 mM in peptide, 0.37 mM in $AgNO_3$) with sodium borohydride (18 mM). But this peptide was not very effective as a stabilizer since it offers to the clusters a chemical lifetime of only 3 days. To overcome this problem other peptides were created. The tested peptides contain 18 amino acids, including D, C and K but also histidine (H) and asparagine (N) or leucine (L). The peptide capable of stabilizing silver clusters during 5 weeks had the sequence "HDCNKDKHDCNKDKHDCN", and the silver clusters produce fluorescence at 630 nm when excited at 400 nm. Giving a closer look to the composition of this peptide, one can notice that it is far from the composition of nucleolin, for instance, it contains three histidines (H) and three cysteines (C) which are minor constituents in nucleolin (∼ 0.1% each) and also three asparagines (N) (∼3% in nucleolin) [63]. Although this peptide and its use as scaffold in the synthesis of silver clusters represent a great advance in the field, the different composition compared to nucleolin, clearly points to the lack of understanding of the basics of cluster synthesis and calls for more exhaustive research to identify both, the mechanism of formation of silver clusters in peptides and the requirements for their stabilization.

A remarkable contribution regarding the use of peptide-protected fluorescent silver clusters in biological systems came with the insertion of fluorescent silver

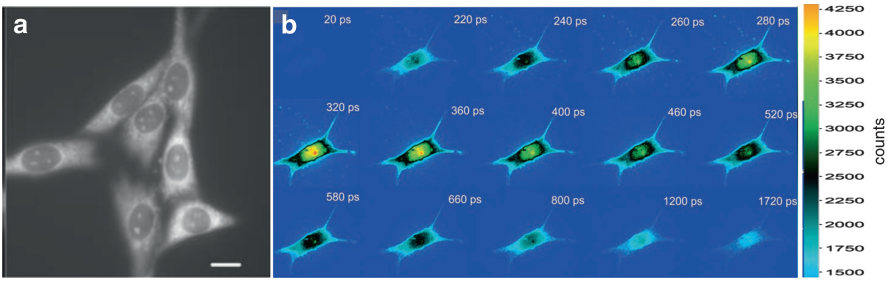

Fig. 10 (**a**) Fluorescence image of methanol-fixed NIH3T3 cells loaded with peptide encapsulated silver clusters for 1 h at room temperature. (**b**) Time profile of the time series images of cell stained with silver nitrate showing the fast silver cluster emission centered in the nucleus at short times with a maximum at 320 nm. Note that *black* indicates an intermediate intensity level in this color scheme [57]

clusters in living cells. Living cells can be loaded with peptide-encapsulated silver clusters even at low temperature, and the cells show evenly distributed silver clusters emission indicating that clusters do not penetrate in the cells by endocytosis. In fixed cells, there is an additional strong staining in the nuclear region (Fig. 10a). The lifetime of silver clusters protected by peptides is similar to the lifetime of fluorescent silver clusters formed in cells, and has two components, one fast of 220 ps (33%) and one slow of 1,760 ps (67%). The fast component allows high signal-to-noise ratio, minimizing contributions from autofluorescence or other added dyes when using picosecond-gated microscopy (Fig. 10b). As a disadvantage, the peptide-encapsulated silver clusters have still relatively low fluorescence quantum yield, about 3% [50].

4.3 Polymers and Dendrimers

The first reported water-soluble fluorescent silver clusters were prepared in dendrimers, by Dickson et al. The combination of second-generation OH-terminated poly(amidoamine) (PAMAM) dendrimer (16 OH per dendrimer) and irradiation with blue light (30 W/cm^2, ~6 s) transforms a 1:3 dendrimer:Ag^+ (OH:Ag^+ 1:0.19) solution into a highly luminescent solution containing silver clusters encapsulated in dendrimers [16]. The silver clusters after more than 30 min of continuous excitation (~500 nm, 300 W/cm^2) keep still about 80% of their fluorescence intensity providing a good photostability. Further studies showed that silver clusters prepared in dendrimers have the similar level of cytotoxicity than that of the corresponding dendrimers. For instance, the NH_2-terminated PAMAM and its succinamic acid-derivative show cytotoxicity only at high concentrations (1 μM), and cells incubated with their silver nanocomposites show intracellular

fluorescence which could make these composites suitable for applications as biomarkers [64] although the composite size is quite large, between 3 and 7 nm. Goodson et al. reported on the fluorescent properties of gold clusters prepared using PAMAM dendrimers [65].

Microgel particles (220 nm) of poly(*N*-isopropylacrylamide-acrylic acid-2-hydroxyethyl acrylate) (poly(NIPAM-AA-HEA)) were used by Kumacheva et al. for the fabrication of fluorescent silver clusters from solutions with molar ratio COOH:Ag of 1:1 and with UV irradiation (365 nm) [66]. The silver clusters present an emission band at 610 nm at the excitation of 450 nm. With control reactions, the authors determined that the presence of PAA (COOH) was decisive for the formation of fluorescent silver clusters, whereas the importance of HEA (OH) was less obvious. Microgels respond to external stimuli like temperature, pH or ionic strength by undergoing noticeable volume changes that influence the optical properties of silver clusters. A high pH ($\sim$8) favors deprotonation of the COOH groups and swollen microgel particles, which lead to a higher emission intensity of the silver clusters. The irradiation conditions were a bit different from the conditions reported in PAMAM: weaker UV source (0.3 W/cm^2) and longer irradiation (minutes) were used here.

Similarly, fluorescent silver clusters could be prepared in so called molecular hydrogels, formed by polyglycerol-*block*-poly(acrylic acid) (PG-*b*-PAA), using a ratio COOH:Ag of 2:1 with UV irradiation (365 nm). The emission band centered at 590 nm reached a maximum after 200 min of irradiation. The authors claim improved photostability of the clusters since they are still luminescent even after 9 h of irradiation, but it has to be mentioned that the irradiation source was weak, only 0.5 mW/cm^2. They claim that it is the number of arms in the star polymer rather than the length of the arms (thus the density of COOH) that plays a crucial role in the formation of silver clusters [30].

In a more simple and cheap way, silver clusters can be prepared in aqueous solutions of commercially available polyelectrolytes, such as poly(methacrylic acid) (PMAA) by photoactivation using visible light [20] or UV light [29]. Ras et al. found that photoactivation with visible light results in fluorescent silver cluster solutions without any noticeable silver nanoparticle impurities, as seen in electron microscopy and from the absence of plasmon absorption bands near 400 nm (Φ_F = 5–6%). It was seen that using PMAA in its acidic form, different ratios Ag^+:MAA (0.15:1–3:1) lead to different emission bands, as discussed in the next section (Fig. 12) [20]. When solutions of PMAA in its sodium form and silver salt were reduced with UV light (365 nm, 8 W), silver nanoclusters were obtained with emission band centered at 620 nm and Φ_F = 18.6%.

As a last example on the fabrication of silver clusters, it is worth mentioning that they can also be prepared in microemulsions, where the small droplets of water act as nanoreactors. The surfactant used was AOT and the reducing agent was a very mild one, i.e. sodium hypophosphite. In this manner, fluorescent silver clusters with less than ten atoms are formed and showed planar shape when deposited onto gold substrates, as determined by scanning tunneling microscopy [67, 68].

4.4 Transfer of Silver Clusters Between Scaffolds

Although many individual biomolecular functions have already been studied by labeling bioactive molecules, proteins, antibodies and DNA strands with organic dyes and quantum dots, the extraordinary properties of silver clusters suggest that these species might be competitive alternatives (Table 1 and Fig. 11a). Nevertheless, silver clusters present some disadvantages in their application to biological systems.

The major issue is the formation of silver clusters in situ in the presence of the biomolecule to be labeled. On one hand, this problem is due to the fact that only a few scaffolds are suitable systems providing the proper environment for the formation of these very small species and preventing the formation of larger silver nanoparticles. On the other hand, the biomolecules might be harmfully

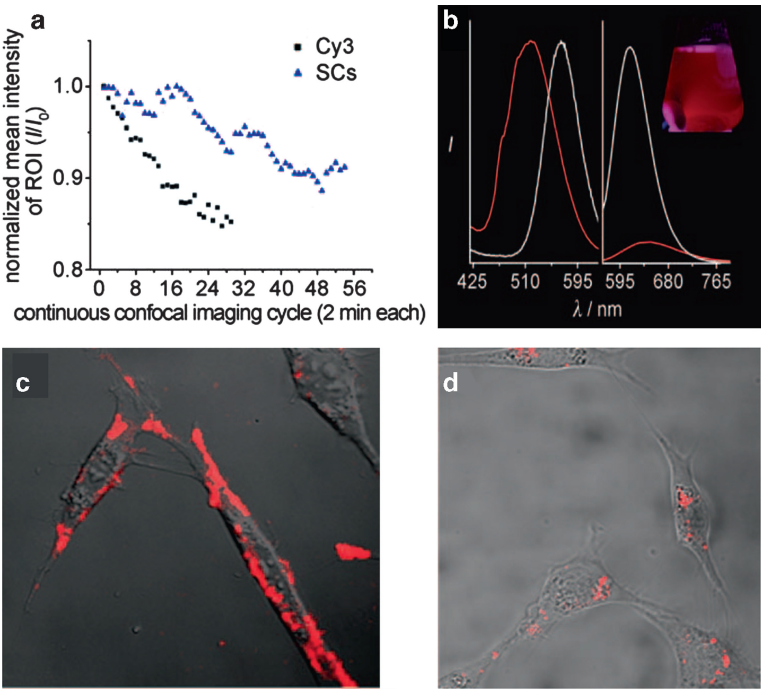

Fig. 11 (**a**) Photostability and comparison between Cy3-labeled and silver clusters-labeled cells under identical staining conditions. (**b**) Silver clusters transferred from PAA to dC_{12}. *Left panel*, normalized excitation spectra of reaction mixture detected at 640 nm before (*red*) and after (*white*) the addition of dC_{12}, which corresponds to individual excitation spectra of PAA-Ag clusters and dC_{12}-Ag clusters, respectively. *Right panel*, tenfold increase in the fluorescence intensity after the addition of dC_{12} (*white*); excited at 545 nm. The *inset* shows PAA-Ag clusters (100 mL) prepared in a Pyrex conical flask, under 354 nm excitation. (**c**)–(**d**) Live NIH 3T3 cells stained with FSP-dC_{24} with silver clusters transfer as the last step. Merge bright-field and silver clusters fluorescence (*pseudo color red*, excited at 543 nm) in cells incubated with FSP-dC_{24} at (**c**) 4°C and (**d**) 37°C [69]

affected during the reduction of silver either by a chemical reductant or by an irradiation source. For example, silver salts can be easily reduced by sodium borohydride, but this reductant may also reduce other functional groups, including disulfide bonds to sulfhydryl groups and could destabilize the folding and function of proteins.

To overcome the difficulty of finding a proper scaffold, which provides the required environment for the formation of silver clusters being at the same time stable during reduction of silver, Dickson et al. proposed a new approach where silver clusters are first prepared using a polymer and then transferred, or shuttled, to the desired biomolecule [69]. These two steps for labeling of cellular components introduce additional advantages to those already mentioned. For instance, the production of silver clusters can be optimized in the first step by adding 3-(2-aminoethylamino)propyltrimethoxy silane (APTMOS) to complex silver ions before stabilization with the proper organic polymer, in this case poly(acrylic acid) (PAA) [69]. The silver clusters prepared in this way have tenfold increased emission intensity (Fig. 11b) and the formation of nanoparticles, was eliminated. In the second step, the transfer efficiency of fluorescent clusters to high-affinity ssDNA sequences (oligocytosines) can be as well optimized for the specific sequence by adjusting the temperature, the pH and the buffer in the transfer step and by varying the ratio of Ag^+/APTMOS in the reduction step.

The shuttle of silver clusters from PAA to oligocytosine due to the stronger interaction of clusters with oligonucleotides was confirmed by a pronounced shift in the excitation spectra from 515 to 570 nm (Fig. 11b). The specific conditions required in each system for the successful shuttle of silver clusters represent an enhancement in the selectivity of the labeling process. Using the cluster transfer, it is possible to produce silver clusters in a polymer and then label ssDNA or oligopeptides [77]. In a similar manner, antibodies conjugated with ssDNA were labeled with fluorescent silver clusters and then the antibody-DNA-Ag clusters were applied to tag live cells. Incubation of live cells at 4°C results in cell-surface staining (Fig. 11c) whereas incubation at 37°C results in internalization of silver clusters and staining inside the cells (Fig. 11d).

The concept of dynamic silver clusters capable to transfer between molecules was also pointed out recently by Ras et al. for silver clusters prepared by photoactivation using PMAA as scaffold [20]. Every specific initial ratio of silver ions to methacrylate unit, Ag^+:MAA, results in distinct spectral bands (Fig. 12a, b). Thus, an initial ratio 0.5:1 gives an absorption band at ~503 nm, whereas a ratio 3:1 gives a band at ~530 nm. The shuttle effect was proven when for a given silver cluster solution with ratio 3:1 and absorption at 530 nm, a blue shift was achieved by the addition of pure PMAA. For instance if the added amount of polymer decreases the ratio Ag^+:MAA from 3:1 to 0.5:1, the new optical band will match exactly with the band corresponding to a solution with initial ratio 0.5:1, that is 503 nm (Fig. 12c). The explanation given for this blue shift was the redistribution of the existent silver clusters in PMAA chains over the newly available PMAA chains, in other words that the clusters shuttle from partly clusters-filled chains to empty ones.

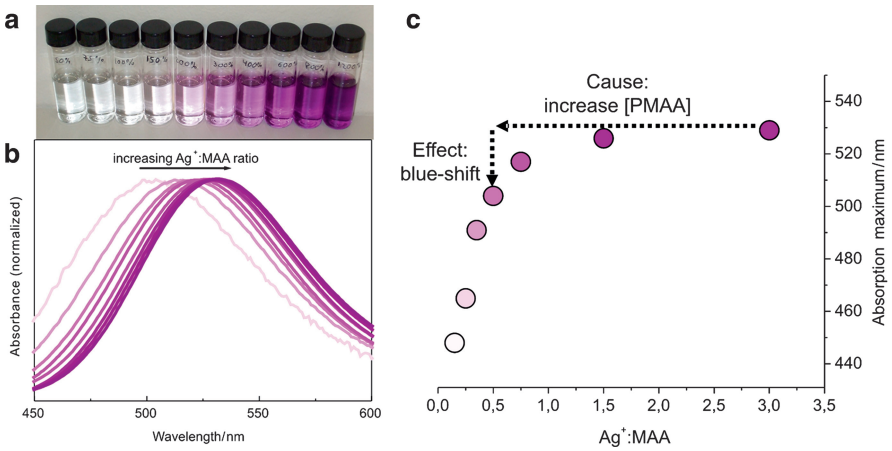

Fig. 12 (**a**) Image of PMAA-protected fluorescent silver clusters prepared with increasing initial ratio Ag^+:MAA from 0.5:1 to 12:1 and equal irradiation time. (**b**) Absorption spectra of the same samples as in (**a**). (**c**) Variation of absorption maxima of some of the samples in (**a**) with molar ratio. *Black arrows* indicate how the absorption band shifts to the blue with the addition of extra polymer to a fluorescent cluster solution explaining the transfer effect of silver clusters among PMAA chains [20]

5 Silver Clusters as Fluorescent Probes for Molecular Sensors

The silver clusters can be applied as fluorescent probes to retrieve information about the chemical environment. There are reported three classes of sensors based on silver clusters. First, we discuss silver cluster sensors of which the fluorescence quenches in the presence of the analyte. Second, we discuss a sensor in which fluorescent clusters are formed only in presence of the analyte. Finally, we discuss the shift in the absorption and fluorescence bands of silver clusters while sensing the chemical environment.

5.1 Quenching

Quenching of silver cluster fluorescence is suitable to detect the presence of small analytes such as cysteine [70] and metal ions [71–73]. Sensing is possible with a low detection limit and high selectivity. Interestingly, Guo et al. show selectivity for Hg^{2+}, not for Cu^{2+} [72], whereas Lan et al. show the selectivity for Cu^{2+}, not for Hg^{2+} [73]. This may seem at first sight a discrepancy; however, both papers use a different DNA sequence leading to a different type of emitter. It shows that the properties of a specific type of silver cluster cannot always be generalized to all silver clusters. Figure 13 shows the case of cysteine detection, in which the silver

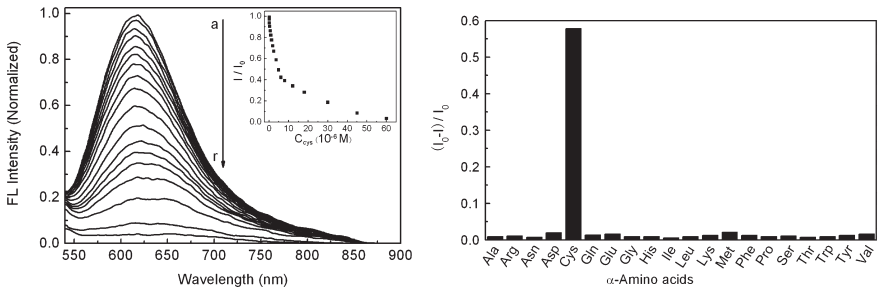

Fig. 13 (*Left*) Emission spectra of PMAA-Ag clusters in the presence of varying concentrations of cysteine from (*a*) 0 to (*r*) 60 $\times$ 10^{-6} M. The *inset* displays the relative fluorescence intensity of Ag clusters recorded at 615 nm vs. the concentration of cysteine. (*Right*) Fluorescence response of Ag clusters in the presence of various α-amino acids [70]

clusters were prepared using PMAA as the scaffold [70]. As shown in Fig. 13, the emission of silver clusters was strongly quenched by cysteine. The quenching exhibited a good linear relationship by Stern–Volmer analysis in the range of 25 nM–6 μM. Other amino acids did not result in fluorescence quenching, demonstrating the excellent selectivity for cysteine detection. The quenching indicates that there is a strong interaction between the clusters and cysteine. Shang and Dong propose that the thiol group of cysteine forms an Ag–S bond followed by oxidation of silver by oxygen, resulting in the quenching of the fluorescence of silver clusters [70].

5.2 *Analyte-Induced Synthesis of Fluorescent Silver Clusters*

The formation of silver clusters is known to be very sensitive to the local environment of the scaffold. For example, we described earlier in this chapter that in case of DNA, the spectral properties depend strongly on the nucleotide sequence (see Table 2). Recently Guo et al. reported on the application of silver clusters to detect single nucleotide mutations in DNA [74]. In their paper they were able to identify the sickle cell anemia mutation in hemoglobin beta chain (HBB) gene. A single-nucleotide mutation (A instead of T) is responsible for the sickle cell disease. They first synthesized a DNA strand (Str-C) that forms a duplex with a normal HBB (Str-B) and has an additional six-base cytosine loop (C_6 loop) at two bases away from the mutation point (See Fig. 14). The C_6 loop is the site where the silver clusters form. When this probe DNA strand was hybridized with the normal HBB gene, it could be used to synthesize intensely fluorescing silver clusters. However, when the probe strand was hybridized with the mutated HBB gene (Str-A), no fluorescence could be detected, indicating that the formation of clusters is prohibited.

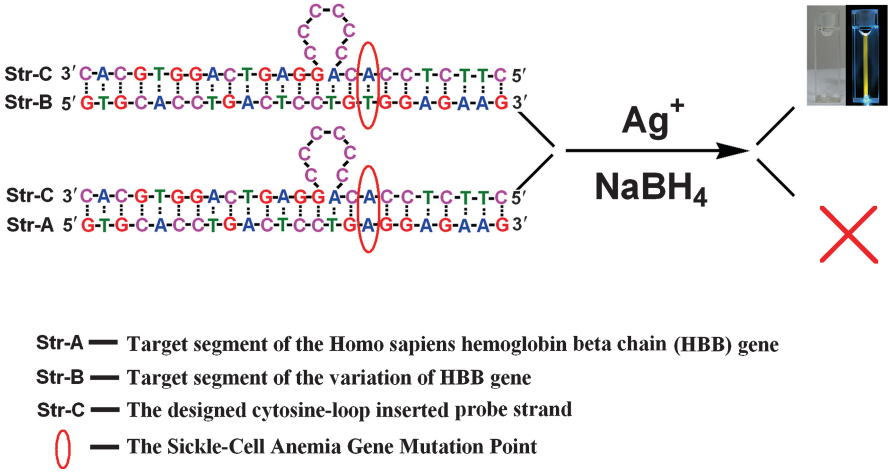

Fig. 14 Use of two different DNA duplexes with inserted cytosine loops working as synthetic scaffolds to generate fluorescent silver clusters for the identification of the sickle cell anemia gene mutation (*black dots* represent hydrogen bonds formed in base pairing and *black dashed lines* the sugar–phosphate backbone) [74]

The duplex with the normal HBB gene has one hydrogen-bonded base pair more than the duplex with the mutated HBB gene, and therefore the first duplex has more double-helical region. The single-nucleotide mismatch has a significant effect on the structure of the duplexes, which in turn strongly influences the local environment where the clusters could form.

5.3 Wavelength-Shifting

Silver clusters change color while sensing their surroundings [20, 75]. Ras et al. have demonstrated that the absorption and emission bands of silver clusters are tunable by changing the chemical environment, such as solvent (Fig. 15) or the relative amount of silver ions (Fig. 12) [20]. In Fig. 15b is shown a photograph of the clusters in a series of water–methanol mixtures. Figure 15c shows the fluorescence of the same samples under UV illumination. The absorption and emission spectra clearly demonstrate a large solvatochromic shift without significant broadening of the spectral bands (Fig. 15d, e). The principles behind the wavelength shift are not yet known. The wavelength-shifting of plasmonic metal nanoparticles forms the basis of localized surface plasmon resonance sensing, a technology which is useful in detecting single molecules of chemical and biological relevance [76]. Analogously, we expect that wavelength-shifting of the fluorescent silver clusters may lead to applications for molecular sensing.

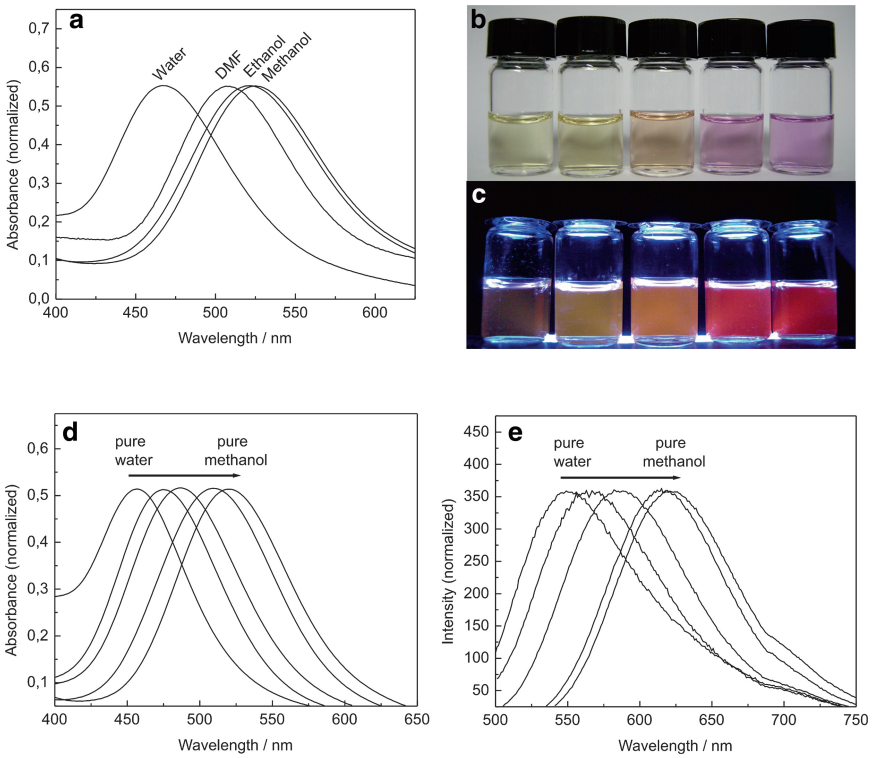

Fig. 15 Color tunability of silver clusters. (**a**) Absorption spectra in various solvents. (**b**) Photograph under visible light and (**c**) under UV light of Ag clusters in water/methanol mixtures, from pure water on the left to pure methanol on the right. (**d**) Absorption and (**e**) emission spectra of the samples imaged in (**b**) [20]

6 Conclusion

Fluorescent silver clusters that are stable in solution are a relatively new class of materials, first reported less than a decade ago. They have optical properties based on electronic transitions between quantized energy levels, resulting in excellent figures of merit including high absorption coefficients and high fluorescence quantum yields. In addition silver clusters have a subnanometer size, are nontoxic, photostable and electrochemiluminescent. Silver clusters are very sensitive to the local environment, which is put into advantage for sensing purposes. However, their sensitivity to local environment also implies that the recipes for silver cluster synthesis are suited only for a specific type of scaffold under specific synthesis conditions and would require optimization to extend the recipe for a different scaffold. In conclusion, fluorescent silver clusters have a unique set of properties making them suitable as fluorescent reporters in labeling and sensing applications, and in future may solve some issues related with organic fluorophores or semiconductor quantum dots.

References

1. Sun T, Seff K (1994) Silver clusters and chemistry in zeolites. Chem Rev 94:857–870
2. Ozin GA, Hugues F, Mattar SM, McIntosh DF (1983) Low nuclearity silver clusters in faujasite-type zeolites: optical spectroscopy, photochemistry and relationship to the photodimerization of alkanes. J Phys Chem 87:3445–3450
3. De Cremer G, Antoku Y, Roeffaers MBJ, Sliwa M, Van Noyen J, Smout S, Hofkens J, De Vos DE, Sels BF, Vosch T (2008) Photoactivation of silver-exchanged zeolite A. Angew Chem Int Ed 47:2813–2816
4. Klotzbücher WE, Ozin GA (1980) Optical spectra of hafnium, tungsten, rhenium and ruthenium atoms and other heavy transition-metal atoms and small clusters (Zr1, 2, Pd1, 2, Au1, 2, 3) in noble-gas matrixes. Inorg Chem 19:3767–3776
5. König L, Rabin I, Schulze W, Ertl G (1996) Chemiluminescence in the agglomeration of metal clusters. Science 274:1353–1355
6. de Lamaestre RE, Bea H, Bernas H, Belloni J, Marignier JL (2007) Irradiation-induced Ag nanocluster nucleation in silicate glasses: analogy with photography. Phys Rev B 76:205431
7. Eichelbaum M, Rademann K, Hoell A, Tatchev DM, Weigel W, Stosser R, Pacchioni G (2008) Photoluminescence of atomic gold and silver particles in soda-lime silicate glasses. Nanotechnology 19:135701
8. Bilan ON, Tyul'nin VA, Cherenda NG, Shendrik AV, Yudin DM (1980) Radiation paramagnetic centers and luminescence centers in silver-doped quartz glasses. J Appl Spectrosc 33:717–720
9. Peyser LA, Vinson AE, Bartko AP, Dickson RM (2001) Photoactivated fluorescence from individual silver nanoclusters. Science 291:103–106
10. Lee T-H, Gonzalez JI, Dickson RM (2002) Strongly enhanced field-dependent single-molecule electroluminescence. Proc Natl Acad Sci USA 99:10272–10275
11. Peyser LA, Lee T-H, Dickson RM (2002) Mechanism of Ag_n nanocluster photoproduction from silver oxide films. J Phys Chem B 106:7725–7728
12. Henglein A, Tausch-Treml R (1981) Optical absorption and catalytic activity of subcolloidal and colloidal silver in aqueous solution: a pulse radiolysis study. J Colloid Interface Sci 80:84–93
13. Ershov BG, Henglein A (1998) Time-resolved investigation of early processes in the reduction of Ag^+ on polyacrylate in aqueous solution. J Phys Chem B 102:10667–10671
14. Linnert T, Mulvaney P, Henglein A, Weller H (1990) Long-lived nonmetallic silver clusters in aqueous-solution – preparation and photolysis. J Am Chem Soc 112:4657–4664
15. Henglein A (1989) Small-particle research – physicochemical properties of extremely small colloidal metal and semiconductor particles. Chem Rev 89:1861–1873
16. Zheng J, Dickson RM (2002) Individual water-soluble dendrimer-encapsulated silver nanodot fluorescence. J Am Chem Soc 124:13982–13983
17. Xu H, Suslick KS (2010) Water-soluble fluorescent silver nanoclusters. Adv Mater 22:1078–1082
18. de Souza N (2007) All that glitters but does not blink. Nat Methods 4:540–540
19. Vosch T, Antoku Y, Hsiang J-C, Richards CI, Gonzalez JI, Dickson RM (2007) Strongly emissive individual DNA-encapsulated Ag nanoclusters as single-molecule fluorophores. Proc Natl Acad Sci 104:12616–12621
20. Díez I, Pusa M, Kulmala S, Jiang H, Walther A, Goldmann AS, Müller AHE, Ikkala O, Ras RHA (2009) Color tunability and electrochemiluminescence of silver nanoclusters. Angew Chem Int Ed 48:2122–2125
21. Ashcroft NW, Mermin ND (1976) Solid state physics. Saunders College, Philadelphia
22. Mohamed MB, Volkov V, Link S, El-Sayed MA (2000) The 'lightning' gold nanorods: fluorescence enhancement of over a million compared to the gold metal. Chem Phys Lett 317:517–523

23. Boyd GT, Yu ZH, Shen YR (1986) Photoinduced luminescence from the noble metals and its enhancement on roughened surfaces. Phys Rev B 33:7923
24. Geddes CD, Parfenov A, Gryczynski I, Lakowicz JR (2003) Luminescent blinking from silver nanostructures. J Phys Chem B 107:9989–9993
25. Zheng J, Nicovich PR, Dickson RM (2007) Highly fluorescent noble-metal quantum dots. Annu Rev Phys Chem 58:409–431
26. Shibu ES, Muhammed MAH, Tsukuda T, Pradeep T (2008) Ligand exchange of $Au_{25}SG_{18}$ leading to functionalized gold clusters: spectroscopy, kinetics, and luminescence. J Phys Chem C 112:12168–12176
27. Richards CI, Hsiang J-C, Senapati D, Patel S, Yu J, Vosch T, Dickson RM (2009) Optically modulated fluorophores for selective fluorescence signal recovery. J Am Chem Soc 131:4619–4621
28. Walter M, Akola J, Lopez-Acevedo O, Jadzinsky PD, Calero G, Ackerson CJ, Whetten RL, Grönbeck H, Häkkinen H (2008) A unified view of ligand-protected gold clusters as superatom complexes. Proc Natl Acad Sci USA 105:9157–9162
29. Shang L, Dong S (2008) Facile preparation of water-soluble fluorescent silver nanoclusters using a polyelectrolyte template. Chem Commun 9:1088–1090
30. Shen Z, Duan H, Frey H (2007) Water-soluble fluorescent ag nanoclusters obtained from multiarm star poly(acrylic acid) as molecular hydrogel templates. Adv Mater 19:349–352
31. Makarava N, Parfenov A, Baskakov IV (2005) Water-soluble hybrid nanoclusters with extra bright and photostable emissions: a new tool for biological imaging. Biophys J 89:572–580
32. Petty JT, Zheng J, Hud NV, Dickson RM (2004) DNA-templated Ag nanocluster formation. J Am Chem Soc 126:5207–5212
33. Stoltenberg RM, Woolley AT (2004) DNA-templated nanowire fabrication. Biomed Microdevices 6:105–111
34. Wei G, Wang L, Liu Z, Song Y, Sun L, Yang T, Li Z (2005) DNA-network-templated self-assembly of silver nanoparticles and their application in surface-enhanced raman scattering. J Phys Chem B 109:23941–23947
35. Kumar A, Ramakrishnan V, Gonnade R, Ganesh KN, Sastry M (2002) Electrostatically entrapped DNA molecules in lipid thin films as templates for the in situ growth of silver nanoparticles. Nanotechnology 13:597
36. Sun L, Wei G, Song Y, Liu Z, Wang L, Li Z (2006) Fabrication of silver nanoparticles ring templated by plasmid DNA. Appl Surf Sci 252:4969–4974
37. Wirges Christian T, Timper J, Fischler M, Sologubenko Alla S, Mayer J, Simon U, Carell T (2009) Controlled nucleation of DNA metallization. Angew Chem Int Ed 48:219–223
38. Yang W, Shen C, Ji Q, An H, Wang J, Liu Q, Zhang Z (2009) Food storage material silver nanoparticles interfere with DNA replication fidelity and bind with DNA. Nanotechnology 20:085102
39. Braun E, Eichen Y, Sivan U, Ben-Yoseph G (1998) DNA-templated assembly and electrode attachment of a conducting silver wire. Nature 391:775–778
40. Izatt RM, Christensen JJ, Rytting JH (1971) Sites and thermodynamic quantities associated with proton and metal ion interaction with ribonucleic acid, deoxyribonucleic acid, and their constituent bases, nucleosides and nucleotides. Chem Rev 71:439–481
41. Eichhorn GL (1973) Inorganic biochemistry. Elsevier Scientific Pub. Co., Amsterdam
42. Marzilli LG (1977) Metal–ion interactions with nucleic acids and nucleic acid derivatives. In: Stephen JL (ed) Progress in inorganic chemistry. Wiley, Hoboken, NJ
43. Yamane T, Davidson N (1962) On the complexing of deoxyribonucleic acid by silver(I). Biochim Biophys Acta (BBA) 55:609–621, Specialized section on nucleic acids and related subjects
44. Luk KFS, Maki AH, Hoover RJ (1975) Studies of heavy metal binding with polynucleotides using optical detection of magnetic resonance. Silver(I) binding. J Am Chem Soc 97:1241–1242
45. Gwinn EG, O'Neill P, Guerrero AJ, Bouwmeester D, Fygenson DK (2008) Sequence-dependent fluorescence of DNA-hosted silver nanoclusters. Adv Mater 20:279–283

46. Richards CI, Choi S, Hsiang J-C, Antoku Y, Vosch T, Bongiorno A, Tzeng Y-L, Dickson RM (2008) Oligonucleotide-stabilized Ag nanocluster fluorophores. J Am Chem Soc 130:5038–5039
47. Patel SA, Richards CI, Hsiang J-C, Dickson RM (2008) Water-soluble Ag nanoclusters exhibit strong two-photon-induced fluorescence. J Am Chem Soc 130:11602–11603
48. Ritchie CM, Johnsen KR, Kiser JR, Antoku Y, Dickson RM, Petty JT (2007) Ag nanocluster formation using a cytosine oligonucleotide template. J Phys Chem C 111:175–181
49. Sengupta B, Ritchie CM, Buckman JG, Johnsen KR, Goodwin PM, Petty JT (2008) Base-directed formation of fluorescent silver clusters. J Phys Chem C 112:18776–18782
50. Yu J, Choi S, Richards CI, Antoku Y, Dickson RM (2008) Live cell surface labeling with fluorescent Ag nanocluster conjugates. Photochem Photobiol 84:1435–1439
51. Dattagupta N, Crothers DM (1981) Solution structural studies of the Ag(I)–DNA complex. Nucl Acids Res 9:2971–2985
52. Arakawa H, Neault JF, Tajmir-Riahi HA (2001) Silver(I) complexes with DNA and RNA studied by Fourier transform infrared spectroscopy and capillary electrophoresis. Biophys J 81:1580–1587
53. O'Neill PR, Velazquez LR, Dunn DG, Gwinn EG, Fygenson DK (2009) Hairpins with poly-C loops stabilize four types of fluorescent Ag_n:DNA. J Phys Chem C 113:4229–4233
54. Kerényi L, Gallyas F (1972) A highly sensitive method for demonstrating proteins in electrophoretic, immunoelectrophoretic and immunodiffusion preparations. Clin Chim Acta 38:465–467
55. Naik RR, Stringer SJ, Agarwal G, Jones SE, Stone MO (2002) Biomimetic synthesis and patterning of silver nanoparticles. Nat Mater 1:169–172
56. Li H, Michael Siu KW, Guevremont R, Le Blanc JCY (1997) Complexes of silver(I) with peptides and proteins as produced in electrospray mass spectrometry. J Am Soc Mass Spectrom 8:781–792
57. Yu J, Patel Sandeep A, Dickson RM (2007) In vitro and intracellular production of peptide-encapsulated fluorescent silver nanoclusters. Angew Chem Int Ed 46:2028–2030
58. Narayanan SS, Pal SK (2008) Structural and functional characterization of luminescent silver–protein nanobioconjugates. J Phys Chem C 112:4874–4879
59. Ayres JG, Crocker JG, Skilbeck NQ (1988) Differentiation of malignant from normal and reactive mesothelial cells by the argyrophil technique for nucleolar organiser region associated proteins. Thorax 43:366–370
60. Giuffrè G, Mormandi F, Barresi V, Bordi C, Tuccari G, Barresi G (2006) Quantity of AgNOR in gastric endocrine carcinoid tumours as a potential prognostic tool. Eur J Histochem 50:45–50
61. Peyser-Capadona L, Zheng J, González JI, Lee T-H, Patel SA, Dickson RM (2005) Nanoparticle-free single molecule anti-stokes Raman spectroscopy. Phys Rev Lett 94:058301
62. Andersson L-O (1972) Study of some silver-thiol complexes and polymers: stoichiometry and optical effects. J Polym Sci Part A 1 Polym Chem 10:1963–1973
63. Srivastava M, Fleming PJ, Pollard HB, Burns AL (1989) Cloning and sequencing of the human nucleolin cDNA. FEBS Lett 250:99–105
64. Lesniak W, Bielinska AU, Sun K, Janczak KW, Shi X, Baker JR, Balogh LP (2005) Silver/dendrimer nanocomposites as biomarkers: fabrication, characterization, in vitro toxicity, and intracellular detection. Nano Lett 5:2123–2130
65. Varnavski O, Ispasoiu RG, Balogh L, Tomalia D, Goodson T III (2001) Ultrafast time-resolved photoluminescence from novel metal–dendrimer nanocomposites. J Chem Phys 114:1962–1965
66. Zhang J, Xu S, Kumacheva E (2005) Photogeneration of fluorescent silver nanoclusters in polymer microgels. Adv Mater 17:2336–2340
67. Ledo A, Martínez F, López-Quintela MA, Rivas J (2007) Synthesis of Ag clusters in micro-emulsions: a time-resolved UV–vis and fluorescence spectroscopy study. Phys B Condens Matter 398:273–277

68. Ledo-Suárez A, Rivas J, Rodríguez-Abreu Carlos F, Rodríguez María J, Pastor E, Hernández-Creus A, Oseroff Saul B, López-Quintela MA (2007) Facile synthesis of stable subnanosized silver clusters in microemulsions. Angew Chem Int Ed 46:8823–8827
69. Yu J, Choi S, Dickson RM (2009) Shuttle-based fluorogenic silver-cluster biolabels. Angew Chem Int Ed 48:318–320
70. Shang L, Dong SJ (2009) Sensitive detection of cysteine based on fluorescent silver clusters. Biosens Bioelectron 24:1569–1573
71. Shang L, Dong SJ (2008) Silver nanocluster-based fluorescent sensors for sensitive detection of Cu(II). J Mater Chem 18:4636–4640
72. Guo W, Yuan J, Wang E (2009) Oligonucleotide-stabilized Ag nanoclusters as novel fluorescence probes for the highly selective and sensitive detection of the Hg^{2+} ion. Chem Commun 23:3395–3397
73. Lan G-Y, Huang C-C, Chang H-T (2010) Silver nanoclusters as fluorescent probes for selective and sensitive detection of copper ions. Chem Commun 46:1257–1259
74. Guo W, Yuan J, Dong Q, Wang E (2010) Highly sequence-dependent formation of fluorescent silver nanoclusters in hybridized DNA duplexes for single nucleotide mutation identification. J Am Chem Soc 132:932–934
75. Patel SA, Cozzuol M, Hales JM, Richards CI, Sartin M, Hsiang JC, Vosch T, Perry JW, Dickson RM (2009) Electron transfer-induced blinking in Ag nanodot fluorescence. J Phys Chem C 113:20264–20270
76. Willets KA, Van Duyne RP (2007) Localized surface plasmon resonance spectroscopy and sensing. Annu Rev Phys Chem 58:267–297
77. Díez I, Hahn H, Ikkala O, Börner HG, Ras RHA (2010) Controlled growth of silver nanoparticle arrays guided by a self-assembled polymer-peptide conjugate. Soft Matter 6:3160–3162
78. Muhammed MAH, Pradeep T (2010) Luminescent quantum clusters of gold as bio-labels. In: AP Demchenko (ed) Advanced Fluorescence Reporters in Chemistry and Biology II, Springer Ser Fluoresc 9:333–353